

## NUMERICAL SIMULATION OF THERMOACOUSTIC REFRIGERATOR

Andreia Aoyagui Nascimento, [andreianascimento@mecanica.ufu.br](mailto:andreianascimento@mecanica.ufu.br)

Francisco Paulo Lépore Neto, [flepore@mecanica.ufu.br](mailto:flepore@mecanica.ufu.br)

Ricardo Fortes de Miranda, [rfmiranda@mecanica.ufu.br](mailto:rfmiranda@mecanica.ufu.br)

Universidade Federal de Uberlândia

Faculdade de Engenharia Mecânica, Uberlândia, Brasil

### Abstract.

*Thermoacoustic is a technology that uses high-amplitude sound waves in a pressurized gas generating a hot and cold region, therefore this device can be used as a heat pump or a refrigerator. This device has the advantage of no ozone-depleting or toxic coolant and few moving parts, because this refrigerator is a system that operates using sound waves to transport heat, therefore its refrigerator is more economic and better for the environment. This refrigerator consists mainly of a closed tube with a stack of a number of parallel plates, and two heat exchangers and a loudspeaker that sustains an acoustic standing wave in the resonator tube. This paper aims to study the performance of a thermoacoustic refrigerator, using the numeric analyze (Ansys –CFX ®), this results is the transient time, and the experimental analyze, was the results at the state steady. The numeric results showed evolution at temperature, pressure and velocity flows are discussed and compared.*

**Keywords:** thermoacoustic, numeric, experimental

### 1. INTRODUCTION

The research on thermoacoustic refrigerators started about 150 years ago, when Lord Rayleigh discussed the possibility of pumping heat with sound. Little further research occurred until Rott's work in 1969.

Thermoacoustic engine is an innovative alternative for cooling, without any moving component, whose potential of high reliability and long life attracting academic and industrial interests (Tang, et al., 2008). These systems operate by using sound waves and non-flammable gases to produce cooling (Newman, et al., 2006).

Thermoacoustic refrigerator consists mainly of a sound source (loudspeaker), that introduces energy in the system, a resonance tube, a porous component called "stack" and two heat exchangers, that provide refrigeration as shown in Fig.1.

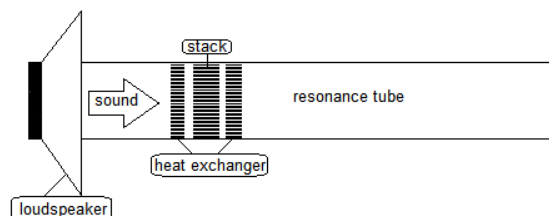


Figure 1. Thermoacoustic system sketch

The thermoacoustic process occurs due to energy deployed from the loudspeaker that moves the fluid (helium, air, and other kind of gas or a mix of them) inside the tube. The sound wave oscillation induces a thermal interaction between gas and wall surface of the stack (Lotton, et al., 2009). The oscillatory pressure wave compresses and expands the gas along the tube, generating at least two different zones of high and low pressure.

Pressure is amplified when the gas passes through the stack core, provoking a thermal interaction between the oscillating gas and the stack surface. This generates an acoustic heat pumping (Tijani et al., 2001). Hence the stack is the heart of the engine, where the thermoacoustic cycle is generated (Tijani, 2003).

The main research in thermoacoustic is focused in order to optimize the system design. Tijani *et al.* in 2002, Wetzel and Herman in 1997 developed the design and optimization of a loudspeaker-driven thermoacoustic refrigerator. The conclusions of these works gave support to improve the design for low-cost thermoacoustic systems (Zontjens, 2005).

Qiu Tu (2003) studied the influence of the stack position, geometry on the thermal gradient produced in the refrigerator. He showed that the stack best configuration is a plate shape, because this geometry is simpler to build, and the better position is at the pressure wave antinode.

Berson, et al. (2008) studied experimentally the characterization of the flow inside a thermoacoustic refrigerator using PIV (particle image velocimetry). Moreover, in this work they studied the oscillation of boundary layers between

two stack plates at high acoustic pressure levels. They observed for the first time the detachment vortices and the symmetry breaking off the vortex street.

Zhanga, et al. (2009) showed the quality factor  $Q$  identification of several types of stack matrix. These results allowed evaluating the stack thermoacoustic performance and helping to choose the most efficient system configuration.

This paper presents show the thermal difference between the stack inside the refrigerator using the different wave frequency, thereunto the experimental model used the plate's stack configuration and fluid air. Computational simulations were conducted using CFX software and their results were compared from model aforementioned.

## 2. THERMOACOUSTIC REFRIGERATION

This section shows the basic principle of thermoacoustic heat pumping mechanism. According to Fig. 1, without the stack, an acoustic source excites the working fluid in the resonant tube generating an acoustic standing wave with wavelength  $\lambda$ .

Considering the resonance tube length equal to  $\lambda/2$ , the resulting pressure and fluid velocity profile result as shown in Fig. 2a.

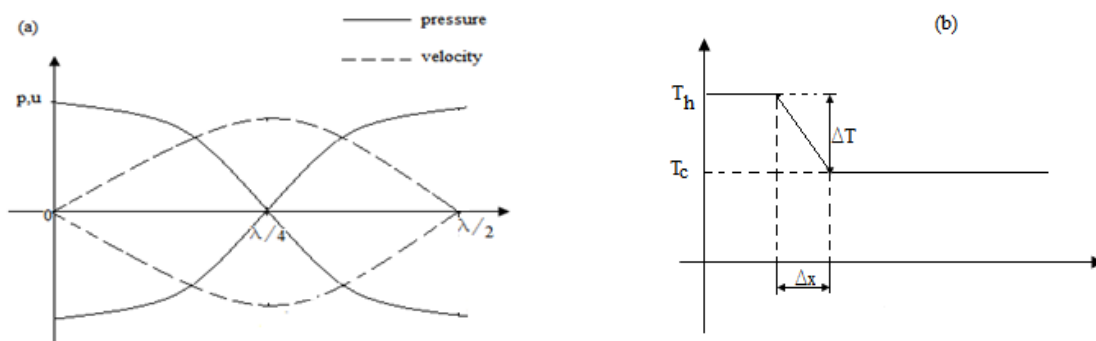


Figure 2. (a) Pressure and velocity (b) Temperature distributions along the resonance tube (Herman, 1997).

Figure 2b shows the temperature distribution when the stack is introduced. The presence of the stack causes a temperature difference ( $\Delta T$ ), along its length ( $\Delta X$ ).

The heat flux generated from the hot to the cold side of the stack is generated by the combination of the compression-expansion effect produced by the acoustic wave (Berson, et al., 2008). This phenomenon obey the thermodynamic Stirling cycle behaviour, that can be seen in Fig. 3, according Swift (1988).

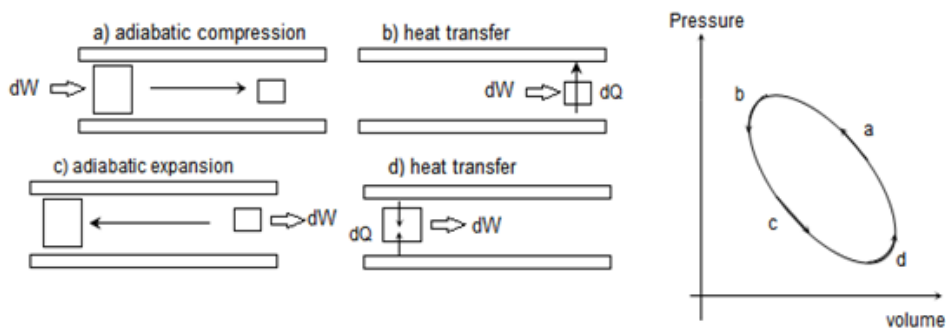


Figure 3. thermodynamic cycle and the acoustic effect inside the stack.

Figure 3 shows a particle inside the stack channel, excited by the pressure wave. On the right graph, region “a” represents the compression phase (the gas moves from the cold to the hot side). At region “b” the fluid particle performs the heat is transferred from the gas to the plate. At region “c” the gas expansion occurs, and the particle moves from the hot to the cold side. Finally at region “d” the particle removes heat from the solid.

The main thermoacoustic parameters are: thermal penetration depth ( $\delta_k$ ) and viscous penetration depth ( $\delta_v$ ) defined by Eq. (1) and Eq. (2).

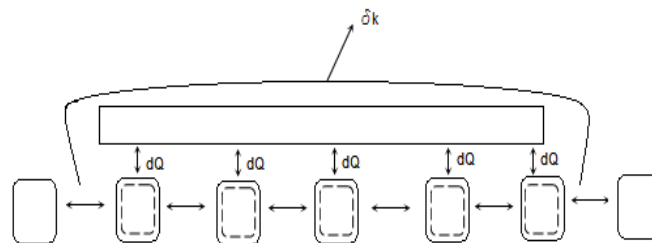


Figure 4. Thermoacoustic effect inside the stack.

The thermoacoustic effect occurs at the thermal penetration depth. It is described as the layer thickness around the stack plate shown by Fig. 4. This thickness roughly corresponds to the distance that heat can diffuse through the fluid during the time interval corresponding to one cycle of oscillation ( $1/f$ ). The losses due to viscous forces occur in the viscous penetration depth. These forces are responsible for the loss of kinetic energy

$$\delta_k = \left( \frac{2k}{\rho_m c_p w} \right)^{\frac{1}{2}} = \left( \frac{2\alpha}{w} \right)^{\frac{1}{2}} \quad (1)$$

$$\delta_v = \left( \frac{2\mu}{\rho_m w} \right)^{\frac{1}{2}} \quad (2)$$

In these equations  $\mu$  is the viscosity,  $\rho_m$  is the density,  $\gamma$ , is the ratio of specific heat,  $k$  is the thermal conductivity and  $c_p$  is the specific heat.

The stack design (length and spacing between the walls) is of crucial importance, because:

- If the plates spacing is too small, the stack will be difficult to build, and the viscous properties of the gas will reduce the sound transmission through the stack.
- If the plates spacing is too large, less gas will be able to transfer heat to the stack plate walls, resulting in lower efficiency.

### 3.MATHEMATICAL FORMULATION

This section shows the mathematical formulation for a thermoacoustic refrigerator. The sound wave frequency generates a pressure with wavelength equal to  $\lambda$ . The refrigerator tube has length equal to  $\lambda/2$ .

The pressure “P” and the velocity and the velocity “U” distributions along the acoustic axis  $x$  in the resonant tube are described as:

$$P = P_m + P_1 e^{i\omega t} \quad (3)$$

$$U = U_1 e^{i\omega t} \quad (4)$$

$P_m$  is the mean pressure,  $P_1$  is the pressure amplitude and  $U_1$  is the velocity amplitude..

Rott's Rott developed the thermoacoustic equation using Eq.( 3) and Eq. (4) to the three conservation equations: momentum, continuity and energy using the thermoacoustic linear theory. Equation (5), is known as the “Rott's Equation”, where  $f_v$ ,  $f_k$  and  $\varepsilon_s$  are Rott's functions,  $a$ , is the sound velocity in the fluid,  $w$ , is the angular velocity,  $\sigma$  is Prandtl number.  $\beta$  is the volumetric expansion, and  $T_m$  is the mean temperature. This equation is presented by Swift (1988).

$$\left[ 1 + \frac{(\gamma - 1)}{(1 + \varepsilon_s)} f_k \right] P_1 + \frac{a^2}{w^2} \rho_m \frac{d}{dx} \left[ \frac{(1 - f_v) dP_1}{\rho_m dx} \right] + \frac{a^2}{w^2} \frac{(f_k - f_v)}{(\sigma - 1)(1 + \varepsilon_s)} \beta \frac{dT_m}{dx} \frac{dP_1}{dx} = 0 \quad (5)$$

The behavior of a thermoacoustic refrigerator can be obtained using the linear steady state theory

#### 4. EXPERIMENTAL ANALYSIS

The thermoacoustic prototype device used by the experimental analysis is shown by Fig. 5. The acoustic excitation is provided by a loudspeaker installed in metallic flange that is connected to the opened end of the resonant tube. The loudspeaker has a diameter equal to 80 mm and is driven by a 50 W electrical power source.

The resonant glass tube external diameter is 24 mm, and its wall thickness is equal to 22 mm. The tube has 230 mm of length and it is closed at the upper end. This geometry defines a quarter wave length, for an excitation frequency of 370 Hz.

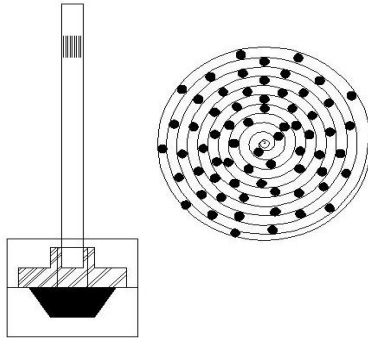


Figure 5. Schematic of the refrigerator and the stack.

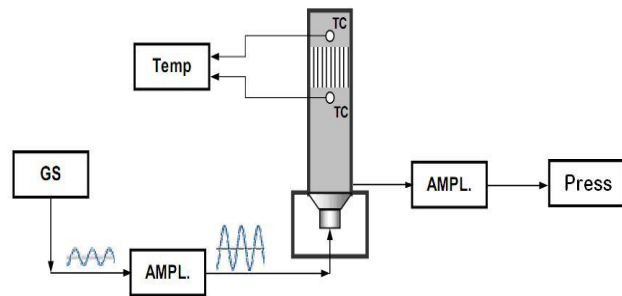


Figure 6. Schematic of experimental bench.

The stack consists of a large number of closely spaced surfaces aligned with tube axis. (A. Russell and Weibulla, 2002). It was built using a sheet of photographic paper with the following characteristics: conductivity of  $\kappa \approx 0.18$  w/m.K at 300 K; thickness of 0.23 mm, and length equal to 35 mm. This sheet was obtained by winding it around a central spindle. The spacing distance between the walls of the film is 0.30 mm. It was set by the nylon spacers shown at the right of Fig. 5. The stack lower end is located at 60 mm from the tube's closed end.

Fig 6 shows the experimental setup. The sine generator (GS) and the power amplifier (AMP) are used to drive the loudspeaker at all frequencies of interest.

Pressure and temperature amplitudes are measured at the hot and cold regions of the refrigerator.

Two type T thermocouples (TC) are installed at 1 mm from each stack's ends. Temperatures are measured by a 12-channel digital instrument, (Scanning thermocouples thermometer)

The pressure transducer (Danfoss MBs 3000) is inserted in the bottom of resonant tube. Transducer signal is amplified and acquired by an oscilloscope.

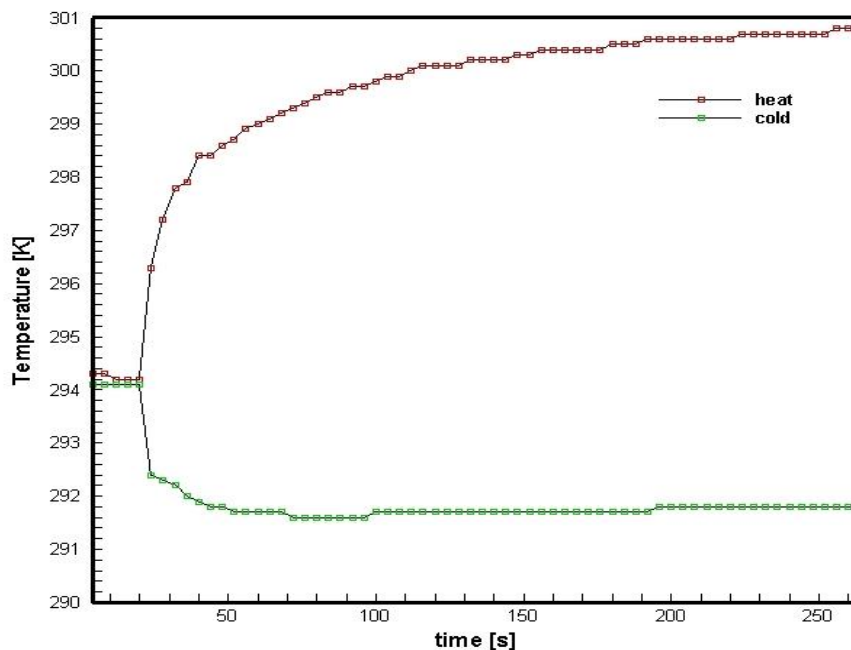


Figure 7. Behavior of experimental temperature to frequency 350 hertz by the time.

Figure 7 shows the temperature evolution along time for 350 Hz wave frequency. The excitation was turned on at  $t = 20$  s. The temperature gradient is higher up to 50 seconds. After the steady state is achieved the temperature difference stabilized around 9 K. The temperature measured by the thermocouple located in the cold region, tends to maintain constant after approximately 100 seconds. After this time the cold region begins to increase this temperature in function of the heat diffusion between the stack. This occurs because this device does not have heat exchanger at the hot and cold region.

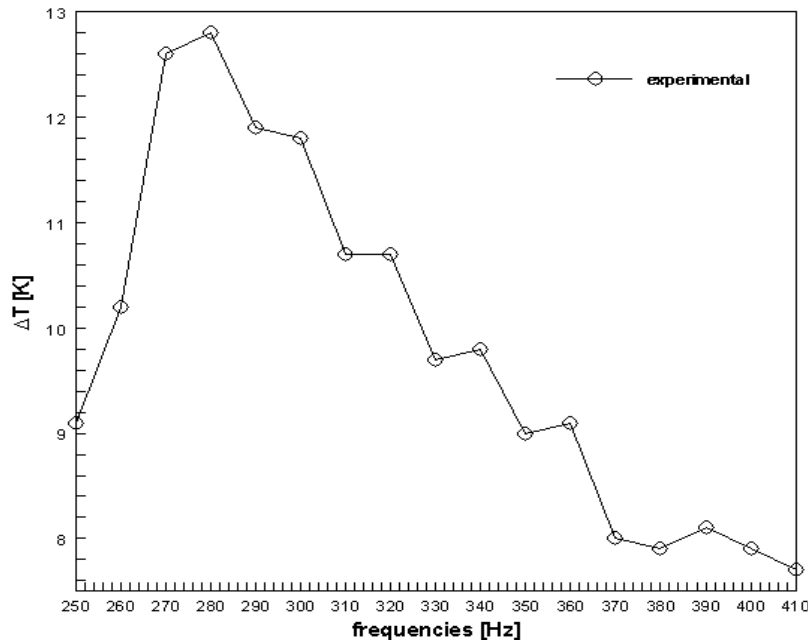


Figure 8 . Experimental Temperature difference  $\Delta T$  in the 250 – 410 Hz frequency band.

Figure 8 shows the experimental temperature difference, at several excitation frequencies. The maximum experimental values of  $\Delta T$  occur at 280 Hz (12.8 K) and also at 270 Hz (12.7 K).

These results don't agree with the refrigerator initial design that imposes the tube's length equal to  $\lambda/4$  (at 370 Hz). This difference may be due to geometric errors and/or to the structural flexibility of the device.

Both models present the same behavior for increasing frequencies: the temperature difference is reduced as the tuning with 370 Hz is lost.

## 6. CFX

The CFX analysis is done using Ansys workbench® to generate the finite element model, which has the following Fig. 9:

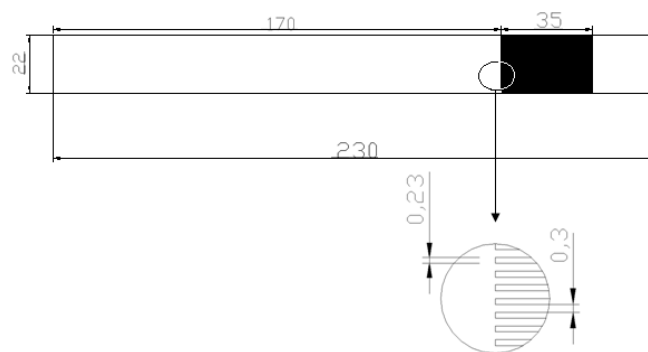


Figure 9. Refrigerator and stack geometry.

Considering the one dimensional sound wave propagation problem, the model has symmetry with respect to both planes XZ and YZ. So, only one quarter of the model has to be constructed, resulting lower computational cost

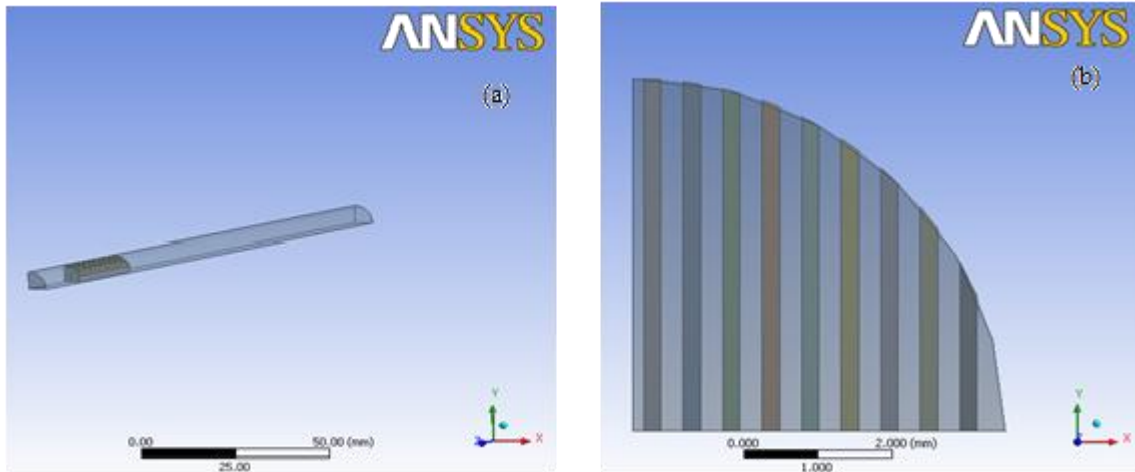


Figure 10. Thermoacoustic refrigerator CFX model and the Stack geometry, used at Ansys Workbench.

The refrigerator and the stack geometry model used by CFX simulation on Ansys® Workbench are shown by Fig. 10. The stack position is the same used on the DeltaEc model and on the experiments. The applied initial conditions and the fixed values imposed on all simulations are:

- reference pressure =  $1 \cdot 10^5$  Pa
- Initial temperature = 293 K
- Frequency = 350 Hz
- Pressure Amplitude=3000 Pa
- Fluid: air
- Stack conductivity = 0.18 w/m.K at 300 K

The model mesh size was set to  $2 \cdot 10^{-3}$  m and the transient solution was carried out using a time step  $\Delta t = 80 \mu s$  within 0.2 seconds time span. The obtained results are: peak amplitude of pressure and velocity time responses along the refrigerator length and the time evolution of the temperature evolution inside the stack

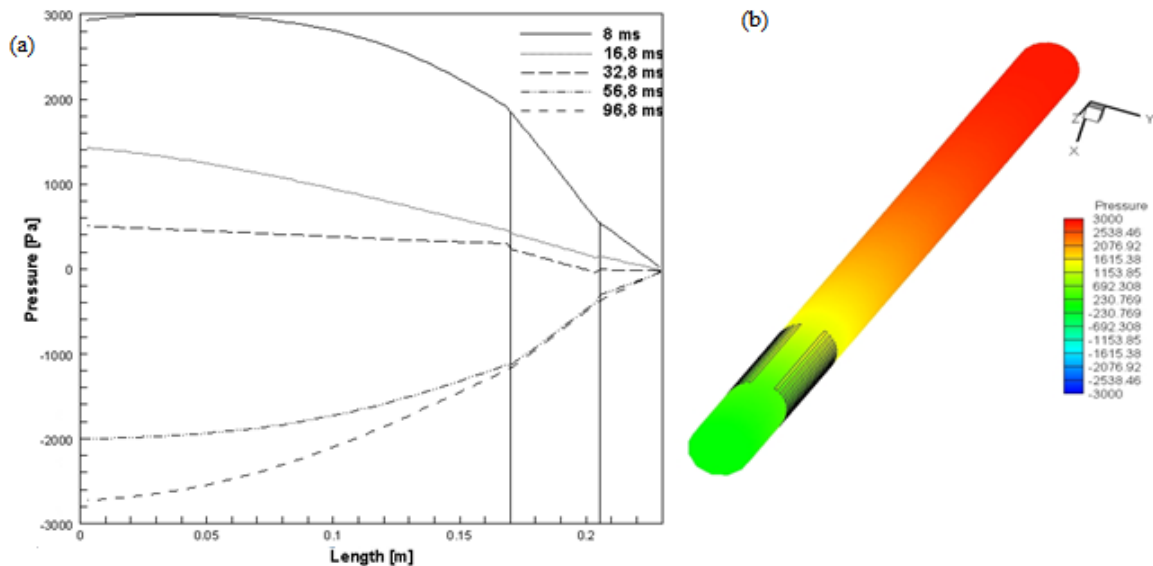


Figure 11. (a) Pressure peak amplitude distribution along the tube length as function of time, (b) Pressure inside the refrigerator for  $t = 192$  ms.

The pressure profile inside the tube at  $t = 0.192$  second is shown by Fig. 11b. The pressure peak amplitude is 3000 Pa at  $x = 0$ . The pressure gradient along the stack length is constant producing a difference about 1000 Pa which is the larger pressure gradient along  $x$ .

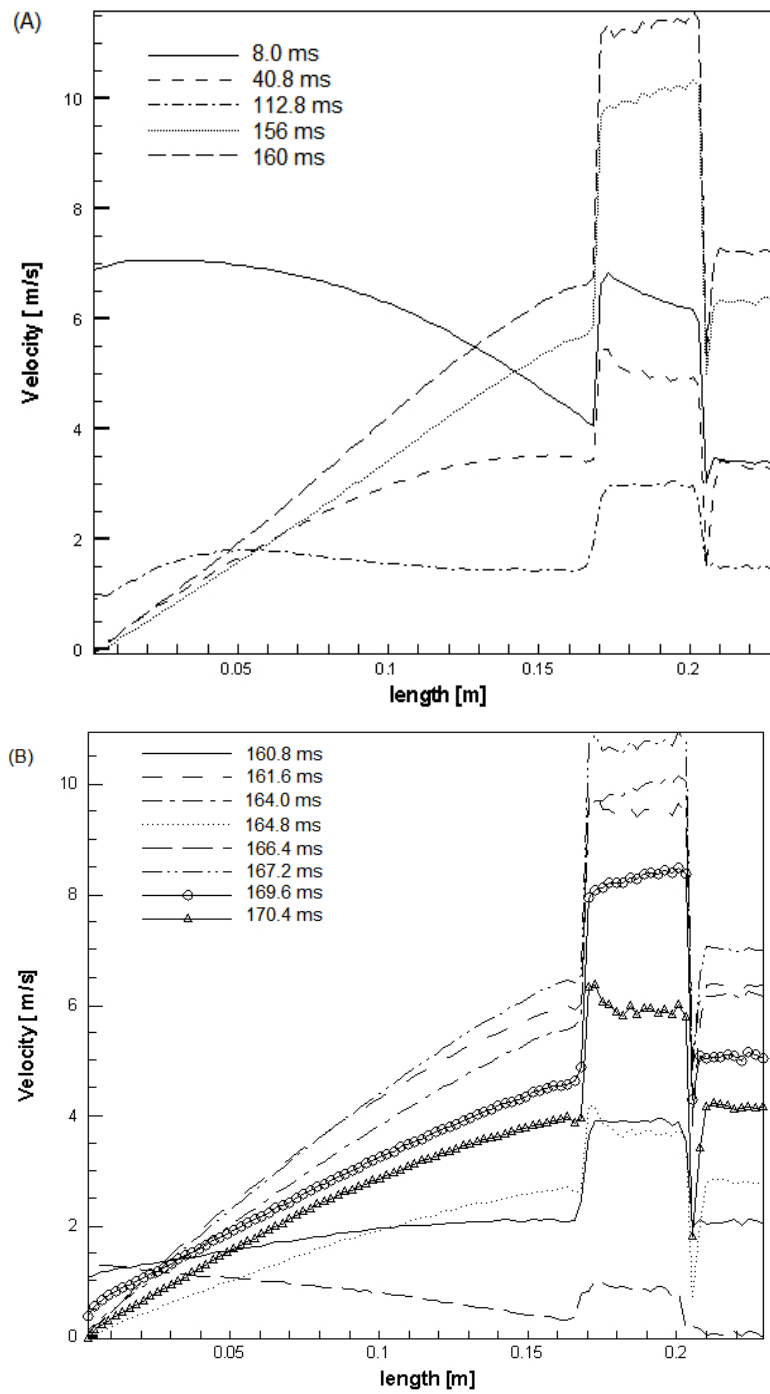


Figure 12. Velocity peak amplitude along the tube length as function of time.

Figure 12 shows the temporal evolution of the axial velocity profile. The flow acceleration is evident at the stack position

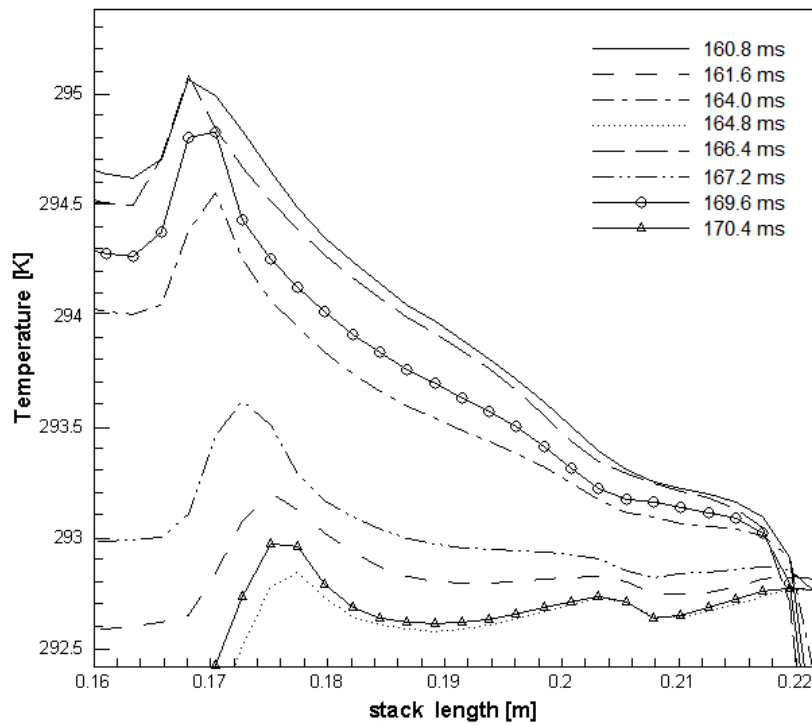


Figure 13. Temperature evolution around the stack length as function of time

Figure 13 shows temporal temperature time evolution along the stack length. This figure shows the region where significant temperature gradient occurs. This is due to the high compression at one side of the stack and the high expansion at the other side.

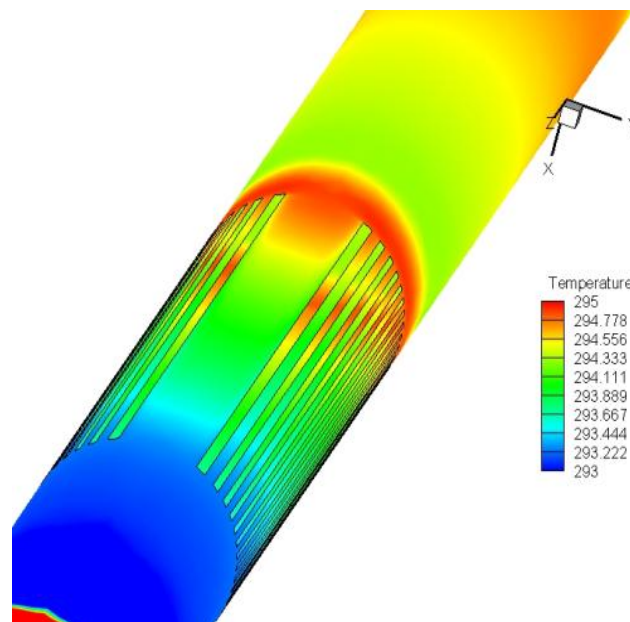


Figure 14 Temperature profile  $t=192$  ms.

Figure 14 represents the temperature profile in the fluid along the stack length calculated at  $t = 192$  m s. The temperature difference is approximately 3 K between the stack extremities.



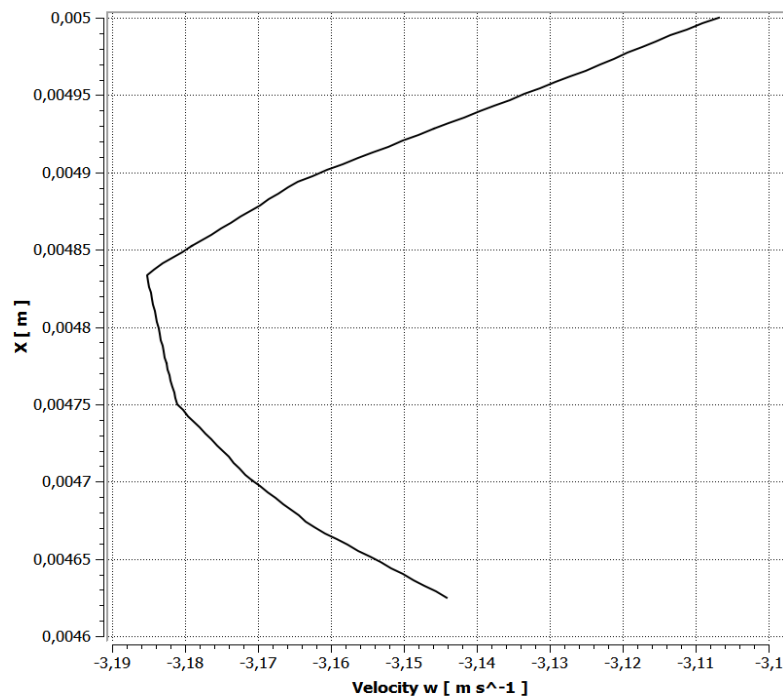


Figure 15-velocity profile inside the porous by CFX simulation.

Figure 15 shows the velocity profile inside the porous at instant which the fluid is expanding. This profile is semi parabolic due to the porosity consist by parallel plates.

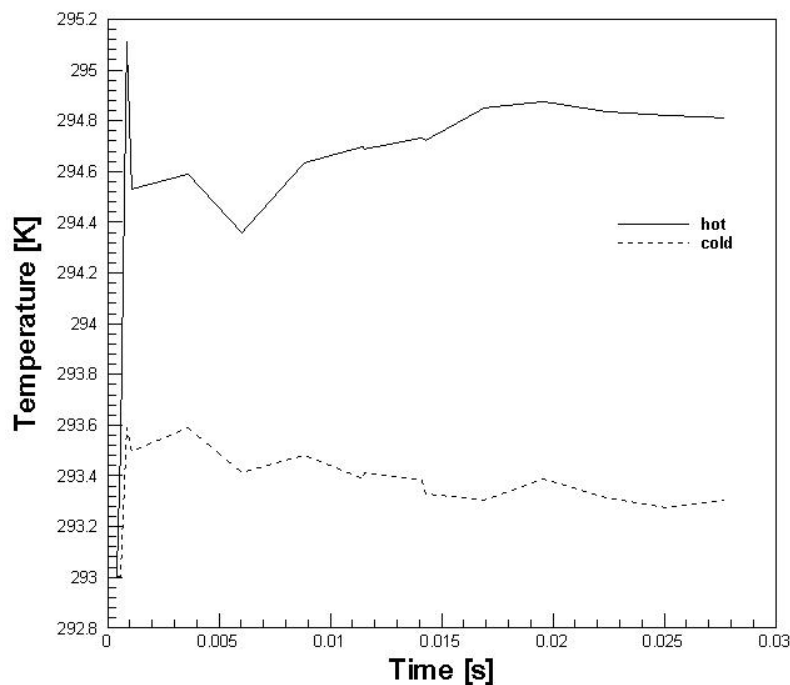


Figure 16 - Behavior of numeric temperature to frequency 350 hertz by the time

Figure 16 shows the temperature evolution along time for 350 Hz wave frequency. Although the small physical time, it allowed noting the curve tendency approximate to Fig.7. The different thermal for time nearly 0.03 s between the sensors located 0.160 m and 0.210 m is 1.0 K.

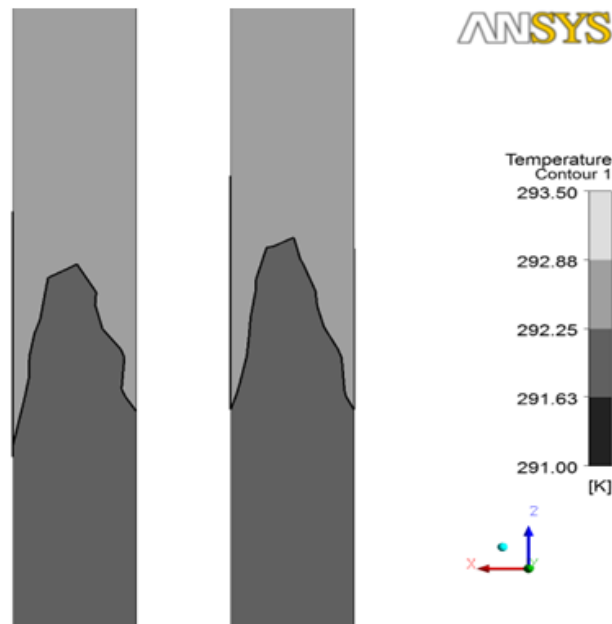


Figure 17- Temperature profile inside the porous by CFX simulation.

Figure 17 shows the temperature profile inside the porous using CFX software. This figure shows the thermal boundary layer is creating, this occurs at 7 ms approximately.

The irregularity at the thermal boundary layer has mesh origin, which has a little node number.

## 7. CONCLUSION

The CFX is good software to analyze the overall phenomena in the thermoacoustic refrigerator, allowing observing the parameters variations as pressure, temperature, velocity and others transitory effects as the pressure oscillation. Therefore it is very important to study effect thermoacoustics inside the porous. But the CFX has few disadvantages as, the high computer cost, i.e. time and memory storage.

Therefore, the cylinder was built using a smaller diameter than experimental it was possible; because the wave is 1-D and the main boundary layer in this phenomenon is inside the stack.

The next steps are testing the other stack positions in the CFX methodology and improve the mesh between the porous in order to study principal part the thermoacoustic refrigerator, furthermore, heat exchanger will be develop, to the experimental model.

## 8. ACKNOWLEDGEMENTS

CAPES, FAPEMIG and CNPQ for financial incentive and Faculdade de Engenharia Mecânica of University Federal de Uberlândia.

## 9. REFERENCES

- A. Russell, Daniel, e Pontus Weibulla. "Tabletop thermoacoustic refrigerator for demonstrations." *American Association of Physics Teachers*, 22 de April de 2002: 1231-1233.
- Berson, Argantheal, Marc Michard, e Philippe Blane-Benon. "Measurement of acoustic velocity in the stack of a thermoacoustic refrigerator using particle image velocimetry." *Heat Mass Transfer*, 2008.
- Lotton, Pierrick, et al. "Transient temperature profile inside thermoacoustic refrigeration." *International Journal of Heat and Mass Transfer*, 2009.
- Luke Zoontjens, Carl Q. Howard, Anthony C. Zander and Ben S. Cazzolato. "Development of a Low-Cost Loudspeaker-Driven Development of a Low-Cost Loudspeaker-Driven." *Proceedings of ACOUSTICS*, 9-11 de November de 2005.
- M.E.H. Tijani, J.C.H. Zeegers, A.T.A.M. de Waele. "Design of thermoacoustic refrigerators." *CRYOGENICS*, DECEMBER de 2001: 49-57.
- Newman, Jonathan, Bob Cariste, Alejandro Queiruga, e Sidney San Martín. "Thermoacoustic Refrigeration." *GSET Research Journal*, 2006.

- Qiu Tu a, \*, Qing Li b, Fangzhong Guo a, Jihao Wu a, Junxia Liu a. "Temperature difference generated in thermo-driven thermoacoustic refrigerator." *CRYOGENICS*, JUNE de 2003: 515-522.
- Swift, G.W. "Thermoacoustic engines." *J Acoust Soc Am*, (1988): 1145-1180.
- Tang, K., Z. J. Huang, T. Jin, e G. B. Chen. "influence of acoustic pressure amplifier dimensions on the performance of a standing-wave thermoacoustic systems." *Applied Thermal Engineering*, 4 de May de 2008: 950-956.
- Tijani, M.E.H., J.C.H. Zeegers, e A.T.A.M. de Waele. "Design of thermoacoustic refrigerators." *CRYOGENICS*, DECEMBER de 2001: 49-57.
- Ward, Bill, John Clark, e Greg Swift. *TUTORIAL - Design Environment for Low-amplitude Thermoacoustic Energy Conversion*. Los Alamos National Laboratory, 2007.
- Zhanga, Chunping, Fangzhong Guoaa, e Xiaoqing Wei Liu. "Quality factor identification for stacks in resonant thermoacoustic system." *IEEE Xplore - digital library*, 2009.

## 10. RESPONSIBILITY NOTICE

The following text, properly adapted to the number of authors, must be included in the last section of the paper:  
The authors are the only responsible for the printed material included in this paper.